

Force-Triggered Control Design for User Intent-Driven Assistive Upper-Limb Robots

Maxime Manzano¹, Sylvain Guégan², Ronan Le Breton², Louise Devigne³ and Marie Babel¹

Abstract— Assistive devices are to be designed with the objective of use in daily-life as well as broad adoption by end users. In this context, it is necessary to tackle usability challenges by properly detecting and acting in accordance to user intents while minimizing the device installation complexity as well. In the case of physical assistive devices, using force/torque sensors is advantageous to detect user intent compared to EMG interfaces, but it remains difficult to correctly translate the detected intent into actuator motions. Focusing on upper-limb assistive robots, the user voluntary force is commonly used with a controller based on an admittance approach which leads to relatively poor reactivity and requires the user to develop force throughout the movement which can lead to fatigue, particularly for people with upper-limb impairments. This work proposes a Force-Triggered (FT) controller which can initiate and maintain movement only from short force impulses. The user voluntary forces are retrieved from total interaction forces by subtracting the passive component measured beforehand during a calibration phase. This paper presents the design of the proposed FT controller and its preliminary testing on pick-and-place tasks compared to an admittance strategy. This experiment was performed with one participant without impairment, equipped with an upper-limb exoskeleton prototype designed from recommendations of physical medicine therapists. This preliminary work highlights the potential of the proposed FT controller. Also, it provides directions for future work and clinical trials with end-users to assess the proposed FT approach usability while used alone or in the form of a hybrid controller between FT and admittance strategies.

Keywords: Assistive robotics, upper-limb, intent detection, force interface, human-robot interaction.

I. INTRODUCTION

Assistive robots are promising technologies to improve the quality of life of people with impairments. In the case of Upper-Limb (UL) assistive robots, the assistance compensates for UL impairment to enable users to gain autonomy [1]. UL assistive devices have already proven their efficiency, significantly improving users ability in Activities of Daily Living (ADLs) [2]. Moreover, assistive robots are well suited for people with severe impairments, as only active devices have shown to improve their performance in ADLs, but still have limited acceptability [3].

Usability, defined by ISO standard 9241 as "the extent to which a product can be used by specified users to achieve specified goals with effectiveness, efficiency and satisfaction in a specified context of use" is a critical factor influencing acceptability [4]. In the context of UL assistance, existing

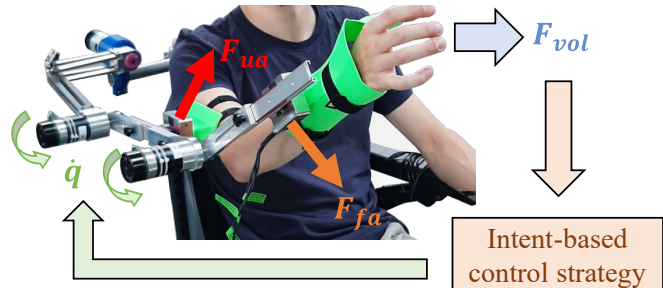


Fig. 1: Usability of the proposed intent-based controller is assessed with a prototype of an UL assistive exoskeleton. User intent is detected by retrieving voluntary forces (F_{vol}) from interaction forces (F_{ua} , F_{fa}) and translated to actuator velocities (\dot{q}) with an intent-based control strategy.

active devices have poor usability as they rely on "very simple push-buttons" [3]. To provide more natural control, many approaches are proposed in the literature [5]. User intent can be detected by e.g. measuring physiological signals such as brain activity [6] or muscle electrical activity [7]. However, these approaches suffer from a lack of robustness to sensor placement, sweat or muscular fatigue [8]. This motivates the use of instrumentation directly embedded in the device, for instance interaction force measurements between the user and the device [9]. However, the latter approach is challenging as potential users with severe impairments may have very little residual force [10].

In the context of UL assistive devices, user intent must be translated into commands for the low-level controller that handles the actuators [11], which is called "mapping" [12]. In the context of force-based intent detection strategies, the force voluntarily developed by the user is retrieved from the total interaction forces with the device. To do so, the interaction force component due to passive UL dynamics must be subtracted from the total measured force. Model-based [13] and measurement-based [14] strategies were proposed to estimate this passive force throughout the UL workspace. As the stiffness of human joints is hard to model [15], we focus on strategies that use a measurement-based method to retrieve user voluntary force, taking joint stiffness into account from the calibration phase. In force-based robots, a very common mapping strategy is Admittance (ADM), which emulates a mechanical system (mass-damper or mass-spring-damper) to convert measured force into actuator motion. However, this strategy has poor reactivity compared to EMG-based controllers [16]. This induces slower motions that can

¹Univ Rennes, INSA Rennes, Inria, CNRS, IRISA - UMR 6074, F-35000 Rennes, France, maxime.manzano@insa-rennes.fr, marie.babel@irisa.fr

²Univ Rennes, INSA Rennes, LGCGM, F-35000 Rennes, France

³Univ Rennes, Inria, CNRS, IRISA, UMR6074, F-35000 Rennes, France

be frustrating and limit user acceptance [17]. Moreover, this strategy requires the user to develop force throughout the movement, which can induce fatigue [18]. To tackle these usability challenges, an alternative mapping strategy to ADM relying on force-based intent detection is needed.

In this paper we propose a Force-Triggered (FT) controller for user intent-driven assistive UL robots. It is designed to facilitate the handling of the robot by initiating or stopping movements with brief force impulses. This user intent-driven controller aims to tackle usability challenges by reducing the force required to initiate and maintain movement, thereby increasing reactivity and reducing fatigue.

Sec. II presents the assistive control framework. Sec. III presents the apparatus to implement the proposed controller with an UL assistive exoskeleton prototype (Fig. 1). Sec. IV presents the controller validation. Finally, Sec. V draws conclusions and guidelines for future work.

II. ASSISTIVE CONTROL FRAMEWORK

The proposed method applies to assistive robots that detect user intent from interaction forces between the device and the user. It relies on a mechanical model of the device and its implementation does not require to model the UL. Indeed, we only consider the physical interfaces as locations of external forces for the assistive robot.

To be generic, we consider that the device is able to measure the interaction forces on the upper-arm and forearm interfaces, respectively called \mathbf{F}_{ua} and \mathbf{F}_{fa} . We assume that these forces are supported by n_a actuators which torques are called $(\tau_i)_{i \in \llbracket 1, n_a \rrbracket}$. The actuator torques required to support the forces developed by the user are computed as

$$\boldsymbol{\tau} = \mathbf{J}_{ua}^T(\mathbf{q})\mathbf{F}_{ua} + \mathbf{J}_{fa}^T(\mathbf{q})\mathbf{F}_{fa}, \quad (1)$$

with $\mathbf{J}_{ua}(\mathbf{q})$ and $\mathbf{J}_{fa}(\mathbf{q})$ the robot Jacobians, respectively linking joint angular velocities to cartesian velocities of the upper-arm and forearm interfaces, $\boldsymbol{\tau} = [\tau_1 \ \tau_2 \ \dots \ \tau_{n_a}]^T$ the actuator torques and $\mathbf{q} = [q_1 \ q_2 \ \dots \ q_{n_a}]^T$ the robot joint angles. To have a more compact form, we rewrite it as

$$\boldsymbol{\tau} = \mathbf{J}^T(\mathbf{q})\mathbf{F} \quad (2)$$

with $\mathbf{J} = \begin{bmatrix} \mathbf{J}_{ua} & \mathbf{0}_{3, n_a} \\ \mathbf{0}_{3, n_a} & \mathbf{J}_{fa} \end{bmatrix}$ and $\mathbf{F} = \begin{bmatrix} \mathbf{F}_{ua} \\ \mathbf{F}_{fa} \end{bmatrix}$.

In this paper, this generic model is applied to an exoskeleton evolving in the sagittal plane, with two actuators assisting shoulder and elbow flexion/extension (Fig. 2).

The proposed control strategy has three levels (Fig. 4): voluntary force retrieving (*i.e.*, intent detection), force mapping to actuator velocity and a low-level speed controller. In this work, the latter is a classical PI controller [11]. The first two levels of the proposed assistive control strategy are described in the following subsections.

A. Retrieving voluntary force

The proposed controller is designed for assistive robots that detect the user intent from \mathbf{F} . The passive forces (called $\mathbf{F}_0(\mathbf{q})$) exerted on the robot while the user is relaxed

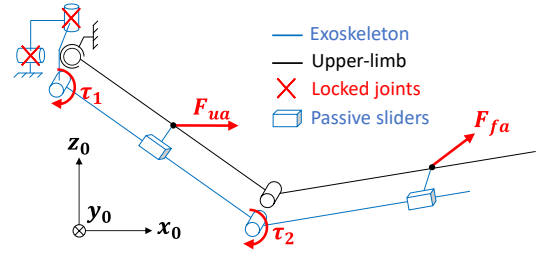


Fig. 2: Mechanical model of the exoskeleton linked to the user at upper-arm and forearm levels. This model is used to compute voluntary torques τ_{vol} from voluntary forces \mathbf{F}_{vol} in the control scheme (see Fig. 4). To keep the UL in the sagittal plane, the two first joints are locked. Passive sliders compensate for joint misalignment.

are removed from \mathbf{F} , so that only the forces voluntarily developed (called \mathbf{F}_{vol}) are retrieved. Thus, the voluntary force \mathbf{F}_{vol} is computed as

$$\mathbf{F}_{vol} = \mathbf{F} - \mathbf{F}_0(\mathbf{q}). \quad (3)$$

with $\mathbf{F}_0(\mathbf{q}) = [\mathbf{F}_{0_{ua}}(\mathbf{q}), \mathbf{F}_{0_{fa}}(\mathbf{q})]^T$, $\mathbf{F}_{0_{ua}}(\mathbf{q})$ and $\mathbf{F}_{0_{fa}}(\mathbf{q})$ being the passive forces of the upper-arm and forearm.

To estimate $\mathbf{F}_0(\mathbf{q})$ throughout the UL workspace, two methods can be used: estimating them from a biomechanical model [13] or measuring them offline during a calibration phase, and then interpolating online [14]. Since joint stiffness of people with UL impairments is hard to model [15], we use a measurement-based method to estimate $\mathbf{F}_0(\mathbf{q})$. For this purpose, a calibration is performed, consisting in measuring interaction forces in different poses while the participant keeps the UL relaxed. The exoskeleton is controlled to reach and stop at 20 poses covering the UL workspace (Fig. 3). We perform this calibration with one participant (see Sec. IV). The results show that the components of $\mathbf{F}_0(\mathbf{q})$ normal to the user segments evolve between -0.71N and -3.2N for the upper-arm and between -2.7N and -3.5N for the forearm throughout the workspace. After this calibration phase, the passive forces $\mathbf{F}_0(\mathbf{q})$ are computed by a linear interpolation between these points.

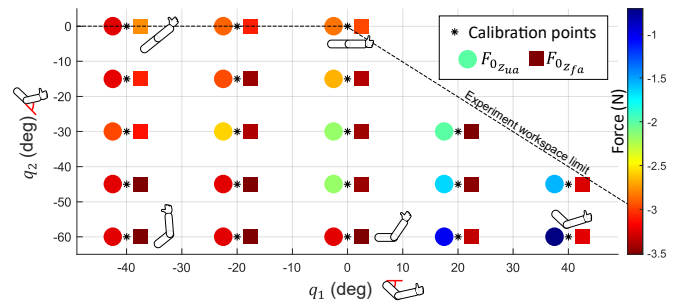


Fig. 3: Joint configurations used to measure $\mathbf{F}_0(\mathbf{q})$. Drawings of the UL illustrate the poses. The workspace is limited for the experiment to avoid self-collisions and collisions with the environment. The results for the components of \mathbf{F}_0 normal to the upper-arm ($F_{0_{zua}}$) and forearm ($F_{0_{zfa}}$) are also shown.

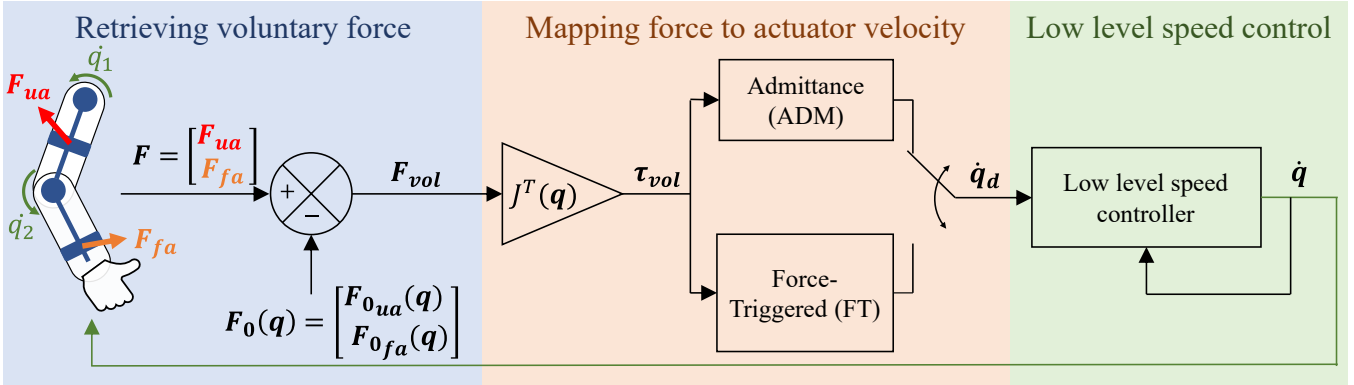


Fig. 4: Architecture of the force-based assistive control. User intent is detected from voluntary forces. This intent is then mapped to actuator velocities with two different strategies: the classical ADM approach or the proposed FT strategy.

B. Mapping force to actuator velocity

The main contribution of this paper lies in the mapping of F_{vol} to speed commands for the low-level controller (\dot{q}_d). In force-based strategies the voluntary torque is computed at the actuator level τ_{vol} from the voluntary force F_{vol} with the transposed Jacobian $J^T(q)$ as in Eq. (2). The classical ADM and the proposed FT strategies are detailed below:

a) *ADM strategy*: It emulates a mass-damper system to filter the voluntary force and converts it into actuator velocities. The ADM transfer function H_{ADM} is given by

$$H_{ADM}(s) = \frac{K}{1 + Ts}, \quad (4)$$

with s the Laplace variable, K the gain and T the time constant of the controller. On each joint, the actuator speed is computed from the voluntary torque with H_{ADM} . Tuning this controller is a trade-off between damping and velocity: high damping (low T) reduces reactivity and continuously slows down movement (leading to fatigue) while low damping (high T) results in slippage, impeding precision tasks. To overcome these limitations, we introduce the FT strategy.

b) *Proposed FT approach*: This strategy has two main objectives: facilitating the initiation of movement and reducing fatigue during movement. It is composed of two states, namely STOP and MOVE (Fig. 5). In the STOP

state, actuator velocities are set to zero ($\dot{q}_d = 0$) so that the UL device maintains its pose. To initiate a movement, the user must develop a voluntary torque $\tau_{i,vol}$ that exceeds a predefined threshold $\tau_{i,th}$ on any of the actuated joint i . This threshold is tuned according to user force abilities such that movement is initiated with as little force as possible, but preventing undesired movement to be triggered. When movement is initiated, the FT controller changes to the MOVE state, where \dot{q}_d is computed as

$$\dot{q}_d = \dot{q}_{d0} \frac{\tau_{vol}}{\max(|\tau_{1,vol}|, |\tau_{2,vol}|, \dots, |\tau_{na,vol}|)} \quad (5)$$

such that the joint with the highest voluntary torque moves at a predefined velocity \dot{q}_{d0} and the others are moving proportionally slower, according to τ_{vol} . \dot{q}_{d0} parameter is tuned according to user preferences. As long as the controller is in the MOVE state, \dot{q}_d is continuously updated according to (5): user can accelerate or decelerate any joint velocities. The movement continues until the user exerts a torque above the threshold in the opposite direction of at least one joint, thus going back to the STOP state. Thus, the user can change the direction of movement of a given joint without triggering the STOP state if the torque exerted does not exceed $\tau_{i,th}$.

III. MATERIALS AND METHOD

An active exoskeleton prototype is used to evaluate the proposed FT controller. The exoskeleton and assistive control implementation are based on guidelines from therapists at the Rehabilitation Center Pôle Saint Hélier in Rennes (France).

A. Exoskeleton prototype

An exoskeleton prototype has been developed to implement the assistive strategies (Fig. 1). This prototype is mounted on a power wheelchair and is designed for 3D movements. In this preliminary work, the exoskeleton is mechanically locked in the sagittal plane, thus assisting shoulder and elbow flexion/extension only. Two Maxon DC motors equipped with hall effect sensors and encoders (EC45Flat, 1:169 and 1:100 gearboxes resp. at shoulder and elbow) are used (Fig. 2). Moreover, two 3-axis force transducers (NF742, Naturoll) are attached at the physical interfaces to

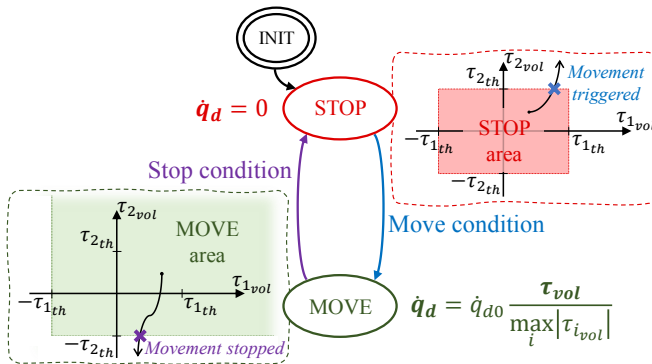


Fig. 5: Working principle of the proposed FT controller used to translate voluntary torques to actuator velocities.

measure F . For this experiment in the sagittal plane, only the forces perpendicular to the limbs are considered to control the exoskeleton. Exoskeleton parts are made of aluminum alloy and lengths are adjustable to align exoskeleton and user joints. The braces are 3D printed and mounted on sliders to eliminate axial forces due to joint misalignment [19]. As a trade-off between complexity and functionality, pronation/supination and wrist rotations are locked with the forearm brace. This choice was made following discussions with occupational therapists. A control board (MicroLabBox, dSpace) is used, communicating via a CAN bus with the low-level controller of the 2 motors (MiniMACS6-AMP-4/50/10, Maxon).

The control parameters have been set to ensure that the actuators run in the same velocity ranges with both FT and ADM strategies. Following the recommendations of therapists, the speed is set slower than natural movements of people without impairments to allow the exoskeleton to be used by people with poor UL motor control. The implemented parameters are listed in Tab. I.

ADM controller		FT controller		
K (rpm.(Nm) $^{-1}$)	T (s)	$\tau_{1_{th}}$ (Nm)	$\tau_{2_{th}}$ (Nm)	\dot{q}_{d0} (rpm)
100	0.8	3	3	250

TABLE I: Parameter values used in the 2 mapping strategies.

The participant has to perform the same pick-and-place tasks in 3 conditions: without wearing the exoskeleton, wearing the exoskeleton with ADM controller, or wearing the exoskeleton with FT controller. In each condition, the participant is asked to perform 4 repetitions of 2 different pick-and-place tasks with a customized object (the object has a cylindrical handle 120mm long, 35mm in diameter and weighs 100g). The order of the tasks is randomized. Both tasks begin with the UL in rest position: upper-arm vertical ($q_1 = 90^\circ$) and forearm horizontal ($q_2 = -90^\circ$). Then, the participant has to take the object on one of the two targets

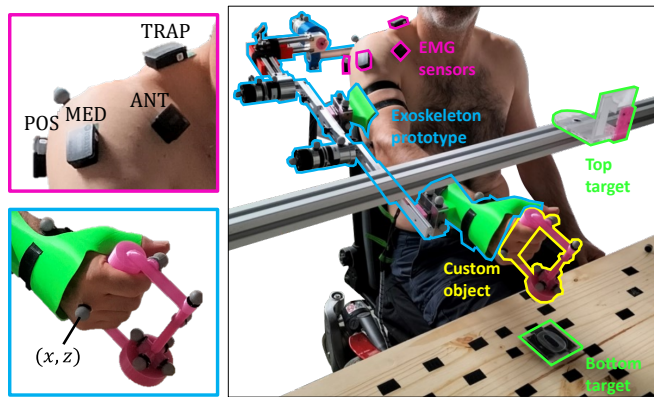


Fig. 6: Right: experimental setup. Top-left: muscle designations (POS: Posterior Deltoid, ANT: Anterior Deltoid, MED: Medial Deltoid, TRAP: Trapezius). Bottom-left: tracking marker for hand trajectories (coordinates (x, z) in the sagittal plane).

and put it on the other one. The tasks are called Bottom-Up (BU) and Top-Down (TD) respectively if the object starts on the bottom or top target. For both control strategies, the participant has as much time as needed to familiarize with the exoskeleton. The only constraint is to perform BU and TD at least once each during the familiarization phase.

In the proposed experimental protocol, the user's hand is tracked using a motion capture system equipped with 4 infrared cameras (Qualisys) to assess task performance. EMG sensors (Trigno, Delsys) are used to measure the activity of 4 muscles of the shoulder. Deltoideus Anterior and Medius are monitored as they are intensively used for arm elevation in ADLs [20]. Deltoideus Posterior is monitored as exoskeletons may lead to an increase in extensor activation [21]. Lastly, the activity of the Trapezius Descendens is measured as prolonged activation of trapezius may lead to neck pain [22]. The sensors are placed following the SENIAM recommendations [23]. The tasks performed without the exoskeleton are used to measure the participant natural motions and also to get reference EMG signals.

B. Data analysis

For all measurements, the tasks are split into four phases, inspired from [24]:

- 1) Reach-For-Grasp (RFG): the participant starts from the rest position and arrives 70mm from the object;
- 2) Grasp (G): the participant ends the RFG motion and grasps the object;
- 3) Transport (T): the participant moves the object from the 1st target and arrives 70mm from the 2nd target;
- 4) Release (R): the participant ends the T motion and releases the object.

EMG signals are used to compute the Mean Effort Index (MEI) [13]. For each muscle m , the Smooth Rectified EMG (SRE) is computed, called $SRE_m(t)$. This envelope of the EMG signal is then normalized using the minimal and maximal values of the SRE measured during the trials without the exoskeleton ($SRE_{\min,m}$ and $SRE_{\max,m}$ respectively). Thus, the normalized SRE of each muscle is computed as

$$nSRE_m(t) = \frac{SRE_m(t) - SRE_{\min,m}}{SRE_{\max,m} - SRE_{\min,m}} \quad (6)$$

The MEI is then computed as the weighted average across the nSRE of the 4 muscles

$$MEI(t) = \frac{1}{\sum_{m=1}^4 w_m} \sum_{m=1}^4 w_m nSRE_m(t) \quad (7)$$

The weights are used so that the muscles that are the most involved in the tasks has higher influence on the MEI, following

$$w_m = 1 - \frac{SRE_{\min,m}}{SRE_{\max,m}} \quad (8)$$

All the SREs were obtained by computing the Root Mean Square (RMS) of a 500ms moving window according to literature recommendations for the study of slow movements [25]. Data are post-processed using Qualisys Track Manager

(QTM) and MATLAB (R2023a) software. The timeline is normalized according to the four phases to compute the mean and Standard Deviation (SD) of the hand trajectory (x, y), the voluntary torque norm ($|\tau_{vol}|$) and MEI.

IV. EXPERIMENTAL RESULTS

To assess the proposed assistive strategy, we conducted a validation experiment following the protocol and data analysis outlined in the previous section. The proposed experiment has been approved by the Operational Committee for the Evaluation of Legal and Ethical Risks (COELER) of the Inria institute. A participant between 30 and 40 years old without UL impairment volunteered to perform experiments

A. Hand trajectory assessment

If the participant managed to perform all pick-and-place tasks with both strategies, the trajectories of the hand vary depending on the experimental conditions. Hence, tasks realized with the exoskeleton lead to larger movements when compared to the one observed without the exoskeleton, in particular when the participant moved away from the upper target. A contrario we observe similar trajectories between FT and ADM strategy conditions (Fig. 7). This suggests that the user adapts its motion pattern to the exoskeleton, preferring caution movements with it than with natural movements, and more constraining its movements in the sagittal plane. Note that this behavior does not affect the efficiency of the task as long as the user remains able to perform the desired movement autonomously. However, it can limit acceptability of the technology.

In terms of movement repeatability, the trajectories with the exoskeleton have highest standard deviations. This is partially explained by the mechanical constraints imposed

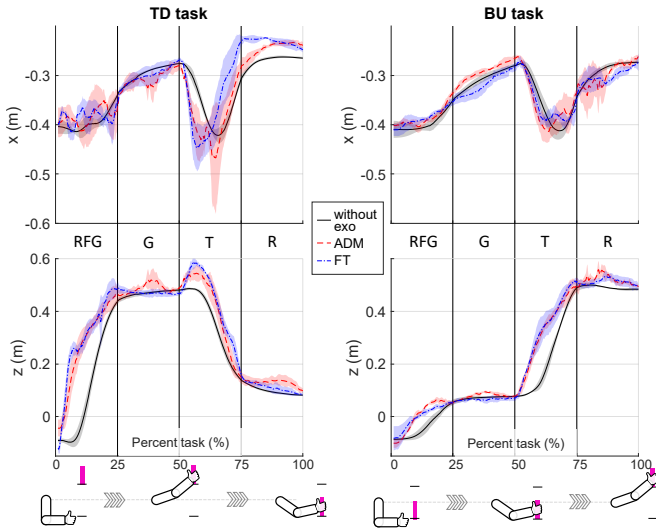


Fig. 7: Trajectories of the hand in the sagittal plane: x (horizontal) and z (vertical) trajectories (mean \pm SD) of the 2 tasks without or with the exoskeleton (2 strategies: ADM and FT). Timelines are split and normalized for the 4 successive phases RFG, G, T, and R (Sec. III-B).

by the exoskeleton locked in the sagittal plane, which leads to less natural movements. In future work, the assistive framework will be assessed for 3D tasks to reach better compatibility between exoskeleton and user kinematics.

B. Usability assessment

For each phase of the two tasks, the voluntary torque norm is computed to evaluate the force developed by the participant to control the exoskeleton (Fig. 8). Apart from the R phase of the TD task, the participant develops with the FT strategy the same amount of forces as with the ADM strategy, or even less. Overall, all ascending motions were performed with less torques. RFG movements demand less torque for both tasks with the proposed FT strategy and with a better repeatability compared to ADM. The same trend is observed for the T phase in the BU task, also ascending. However, downward movements show similar torque norms with both strategies as shown on the T phase of the TD task.

Focusing on precision tasks (*i.e.*, G and R phases), no systematic trend is observed. The precision tasks near the top target (G phase of TD task and R phase of BU task) show similar torque norm values. However, precision tasks near the bottom target are contradictory. Indeed, the torque norm with the FT strategy was lower than with the ADM strategy in the G phase of the BU task, but worse in the R phase of the TD task with much higher mean and SD.

This shows that the proposed FT controller is promising

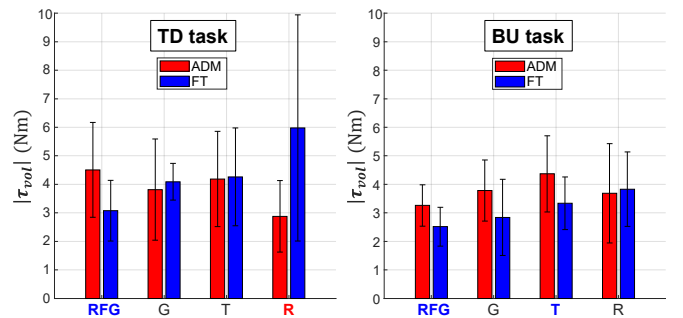


Fig. 8: Comparison of the voluntary torque norm between both strategies for each task (mean \pm SD). Each phase name is colored in blue (resp. red) if FT strategy (resp. ADM) performs best. FT is considered better than ADM when $(|\tau_{vol}| + SD)_{FT} < |\tau_{vol}|_{ADM}$ and conversely.

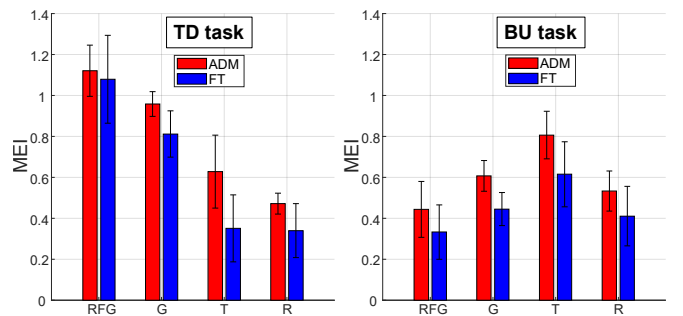


Fig. 9: Comparison of the MEI between both strategies for each task (mean \pm SD).

for enhancing usability during reaching and transport phases, where no precise interactions with the environment are required. However, ADM control may be more appropriate for precision tasks as joint velocities can be continuously and proportionally controlled by the user in any direction. Here, if no clear conclusion can be derived from the results, future work will investigate how this trend is observed in a wider population, including individuals with UL deficiencies. In addition, as FT and ADM controllers seem complementary, a hybrid controller switching between the two strategy depending on the task phase will be developed and assessed.

Focusing on muscular activity, the participant MEI is lower with the FT controller compared to ADM in all phases of both tasks (Fig. 9). This is an encouraging feature for reducing user fatigue during prolonged use of the assistive robot: this assertion will be studied in future works.

V. CONCLUSION AND PERSPECTIVES

This paper proposes a Force-Triggered (FT) control method to improve the usability of assistive robots that detect user intent through interaction forces. The novelty of the method lies in the way the controller converts the user intent into motion commands for the actuators. Indeed, the classical admittance method (ADM) suffers from poor reactivity and induces fatigue. Instead, our method initiates and stops movements from only short force impulses.

This FT controller was compared to the classical ADM controller through an experiment with one participant without UL impairment. Preliminary results observed during pick-and-place tasks validate the proposed strategy. Interestingly, new motion patterns and hand trajectories are observed with the exoskeleton compared to motions without it, similarly with FT and ADM controllers. The proposed FT controller is particularly relevant during reaching and transport phases. Indeed, the participant operated the assistive robot with lower torque values during these phases compared to the trials with the ADM controller. However, ADM controller seems more appropriate for precision tasks as the user can modulate joint velocities without stopping the device. Nevertheless, the participant exhibited lower muscle activity with the FT controller during all phases of the tasks, which is promising for reducing fatigue during long-term use of the device. This preliminary work shows the relevance of a hybrid controller, switching between the proposed FT and ADM strategies depending on the task phase. In future works, we will involve more participants in experiments to check the robustness of FT controller against user variability.

ACKNOWLEDGMENT

Authors would like to thank Charles Pontonnier (Inria/IRISA), Quentin Da-Silva, Eric Bazin, Fabien Grzeskowiak, and Sébastien Thomas from INSA Rennes.

REFERENCES

- [1] M. A. Gull, S. Bai, and T. Bak, "A Review on Design of Upper Limb Exoskeletons," *Robotics*, vol. 9, no. 1, p. 16, 2020.
- [2] M. Gandolla *et al.*, "The Effectiveness of Wearable Upper Limb Assistive Devices in Degenerative Neuromuscular Diseases," *Front. Bioeng. Biotechnol.*, vol. 7, p. 450, Jan. 2020.
- [3] V. Longatelli *et al.*, "User-centred assistive SystEm for arm Functions in neUromuscuLar subjects (USEFUL): a randomized controlled study," *J NeuroEngineering Rehabil*, vol. 18, no. 1, p. 4, 2021.
- [4] H.-C. Kim, "Acceptability Engineering: the Study of user Acceptance of Innovative Technologies," *Journal of Applied Research and Technology. JART*, vol. 13, no. 2, pp. 230–237, Apr. 2015.
- [5] J. Gantenbein *et al.*, "Intention Detection Strategies for Robotic Upper-Limb Orthoses," *Front. Neurobot.*, vol. 16, p. 815693, 2022.
- [6] A. Kapsalyamov *et al.*, "Brain-computer interface and assist-as-needed model for upper limb robotic arm," *Advances in Mechanical Engineering*, vol. 11, no. 9, p. 1687814019875537, Sep. 2019.
- [7] B. Treussart *et al.*, "Controlling an upper-limb exoskeleton by EMG signal while carrying unknown load," in *2020 IEEE Int. Conference on Robotics and Automation (ICRA)*, May 2020, pp. 9107–9113.
- [8] H. K. Hameed *et al.*, "A Review on Surface Electromyography-Controlled Hand Robotic Devices Used for Rehabilitation and Assistance in Activities of Daily Living," *JPO: Journal of Prosthetics and Orthotics*, vol. 32, no. 1, p. 3, Jan. 2020.
- [9] P. N. Kooren *et al.*, "Design and control of the Active A-Gear: A wearable 5 DOF arm exoskeleton for adults with Duchenne muscular dystrophy," in *2016 6th IEEE International Conference on Biomedical Robotics and Biomechanics (BioRob)*, Jun., pp. 637–642.
- [10] M. Gandolla *et al.*, "An assistive upper-limb exoskeleton controlled by multi-modal interfaces for severely impaired patients: development and experimental assessment," *Robotics and Autonomous Systems*, vol. 143, p. 103822, Sep. 2021.
- [11] T. Desplenter *et al.*, "Rehabilitative and assistive wearable mechatronic upper-limb devices: A review," *J NeuroEngineering Rehabil*, vol. 7, p. 2055668320917870, Jan. 2020.
- [12] M. R. Tucker *et al.*, "Control strategies for active lower extremity prosthetics and orthotics: a review," *J NeuroEngineering Rehabil*, vol. 12, no. 1, p. 1, Jan. 2015.
- [13] F. Just *et al.*, "Human arm weight compensation in rehabilitation robotics: efficacy of three distinct methods," *J NeuroEngineering Rehabil*, vol. 17, no. 1, p. 13, 2020.
- [14] J. Lobo-Prat *et al.*, "Implementation of EMG- and Force-Based Control Interfaces in Active Elbow Supports for Men With Duchenne Muscular Dystrophy," *IEEE Transactions on Neural Systems and Rehabilitation Engineering*, vol. 24, no. 11, pp. 1179–1190, Nov. 2016.
- [15] D. Ragonesi *et al.*, "Quantifying Anti-Gravity Torques for the Design of a Powered Exoskeleton," *IEEE Transactions on Neural Systems and Rehabilitation Engineering*, vol. 21, no. 2, pp. 283–288, Mar. 2013.
- [16] J. Lobo-Prat *et al.*, "Evaluation of EMG, force and joystick as control interfaces for active arm supports," *J NeuroEngineering Rehabil*, vol. 11, no. 1, p. 68, Apr. 2014.
- [17] M. Mathew *et al.*, "A systematic review of technological advancements in signal sensing, actuation, control and training methods in robotic exoskeletons for rehabilitation," *Industrial Robot: the Int. J. of robotics research and application*, vol. 50, no. 3, pp. 432–455, Jan. 2022.
- [18] M. Mashayekhi and M. M. Moghaddam, "EMG- biased Fatigue Adaptation in Admittance Control of Hand Rehabilitation," in *2019 7th International Conference on Robotics and Mechatronics (ICRoM)*, Nov. 2019, pp. 487–491.
- [19] R. Mallat *et al.*, "Human-Exoskeleton Joint Misalignment," in *2019 Int. Conf. on Advances in Biomedical Engineering*, Oct. 2019, pp. 1–4.
- [20] D. H. Hawkes *et al.*, "Normal shoulder muscular activation and coordination during a shoulder elevation task based on activities of daily living: An electromyographic study," *Journal of Orthopaedic Research*, vol. 30, no. 1, pp. 53–60, 2012.
- [21] M. Musso, A. S. Oliveira, and S. Bai, "Influence of an upper limb exoskeleton on muscle activity during various construction and manufacturing tasks," *Applied Ergonomics*, vol. 114, Jan. 2024.
- [22] C. NICOLETTI and T. LÁUBLI, "Trapezius muscle activity and body movement at the beginning and the end of a workday and during the lunch period in female office employees," *Industrial Health*, vol. 55, no. 2, pp. 162–172, Mar. 2017.
- [23] H. J. Hermens *et al.*, "European recommendations for surface electromyography," *Roessingh research and development*, vol. 8, no. 2, pp. 13–54, 1999, publisher: Chicago.
- [24] N. Valè *et al.*, "Characterization of Upper Limb Impairments at Body Function, Activity, and Participation in Persons With Multiple Sclerosis by Behavioral and EMG Assessment," *Front Neurol*, vol. 10, p. 1395, 2019.
- [25] P. Konrad, "The abc of emg," *A practical introduction to kinesiological electromyography*, vol. 1, no. 2005, pp. 30–5, 2005.